Journal of Electronic Research and Application, 2026, Volume 10, Issue 5
http://ojs.bbwpublisher.com/index.php/JERA
Online ISSN: 2208-3510
Print ISSN: 2208-3502

Optimization of Welding Sequence for Bridge Crane Girder Structure Based on Numerical Simulation

Mingyuan Li*, Peiyun Yue, Yufei Yan, Siqun Ma

Zhan Tianyou College of Dalian Jiaotong University(CRRC College), Dalian 116028, Liaoning, China

***Corresponding author*:** Mingyuan Li, 2685575101@qq.com

Abstract: Bridge cranes are key equipment in modern industry and logistics. Their manufacturing quality directly affects the safety and service life of the entire machine. The main girders and end beams of such cranes are typically fabricated by welding thick plates. Residual stress and deformation generated during welding are major factors that influence the structural service life and load-bearing capacity. The paper adopts the inherent strain method as the core theory. A mid-surface model of the structure is created using SolidWorks. Two-dimensional mesh discretization and geometry cleanup are performed in Hypermesh. Finally, numerical simulations of different welding sequence schemes are carried out using Sysweld software. During the research, the double ellipsoid heat source model is first calibrated and validated for T-welded joints to ensure the accuracy and applicability of the heat source parameters. Subsequently, simulations are performed according to different welding sequence schemes. Residual stress distribution contours and deformation contours under each scheme are extracted, and a quantitative comparative analysis is conducted on the maximum residual stress, deformations in each direction, and total deformation, leading to the selection of an optimal welding sequence scheme. The simulation results show that different welding sequences have a significant effect on the final residual stress and deformation distribution. Improving the welding sequence can effectively control welding-induced residual stress and deformation, providing guidance for optimizing the welding process of bridge cranes.

Keywords: Bridge crane; Bridge frame structure; Residual deformation; Welding sequence

Online publication: Jun 29, 2026

1. Introduction

Bridge cranes are among the most common and widely used hoisting machines in industry. Their main functions are vertical lifting and horizontal movement of heavy loads. A bridge crane typically consists of a bridge frame structure, a crane traveling mechanism, a trolley traveling mechanism, a hoisting mechanism, and an electrical control system. Among these, the bridge frame structure is the main load-bearing

component. It bears the weight of the lifted load, the self-weight of the structure, and various dynamic and wind loads [1]. The strength, stiffness, and stability of the bridge frame directly determine the safety and service life of the crane. Since the structure is mostly assembled by welding steel plates, the quality of welding is directly related to the reliability of the entire crane.

Welding is an efficient and reliable metal joining method widely used in crane manufacturing. The welding process is inherently complex, involving the coupled effects of multiple physical fields such as heat transfer, phase transformation, and thermal elastoplastic deformation. Under the localized, intense heating of the welding heat source, the weld and its surrounding areas undergo rapid heating, melting, cooling, and solidification. This non-uniform temperature field leads to uneven thermal expansion and contraction, which in turn generates welding residual stress and welding deformation in the structure [2]. By establishing a reasonable finite element model and setting accurate boundary conditions and heat source parameters, the thermomechanical behavior during welding can be simulated. This allows for predicting the distribution patterns of welding residual stress and deformation, thereby enabling rapid evaluation and optimization of different welding sequences.

2. Research content

The paper takes the bridge frame structure of a bridge crane as the research object. The structure consists of two parallel main beams and end beams at both ends, as shown in **Figure 1**. The main beam is the primary component carrying the lifting load. It usually adopts a box-section structure, consisting of a top cover plate, a bottom cover plate, two web plates, and internal stiffener plates. The end beams connect the two main beams and transfer the entire crane load to the crane traveling mechanism [3]. The material of the bridge frame is Q345 steel. The welding method is CO_2 gas shielded arc welding, with two layers and two passes per weld.

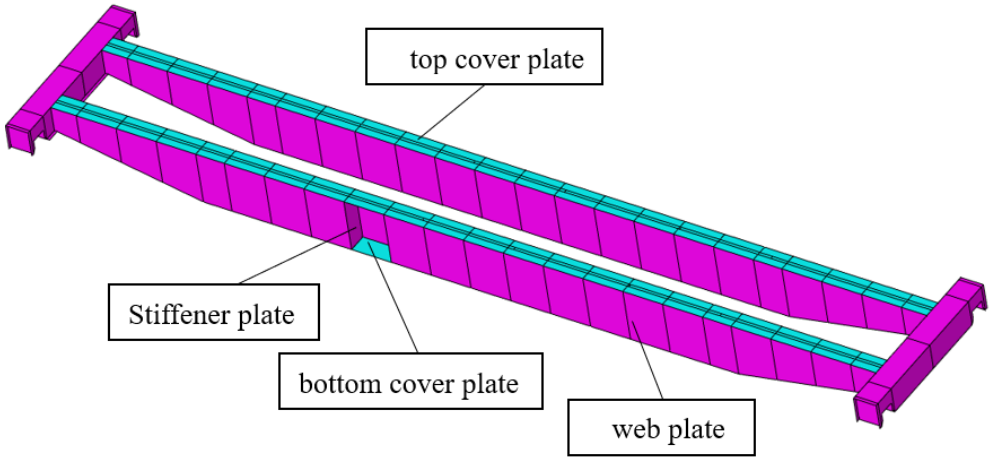

Figure 1. Bridge frame structure model.

In the bridge frame structure, there are numerous and densely distributed welds. These mainly include the fillet welds between the upper cover plate and the webs, between the upper cover plate and the stiffeners, between the webs and the stiffeners, and between the lower cover plate and both the webs and stiffeners. A portion of the main girder structure is selected to illustrate the weld arrangement, as shown in **Figure 2**.

Considering the symmetry of the structure and the regularity of weld distribution, appropriate simplifications are made to the model to ensure computational accuracy. Process features such as rounded corners and chamfers, which have negligible effects on the analysis of welding residual stress, are neglected [4].

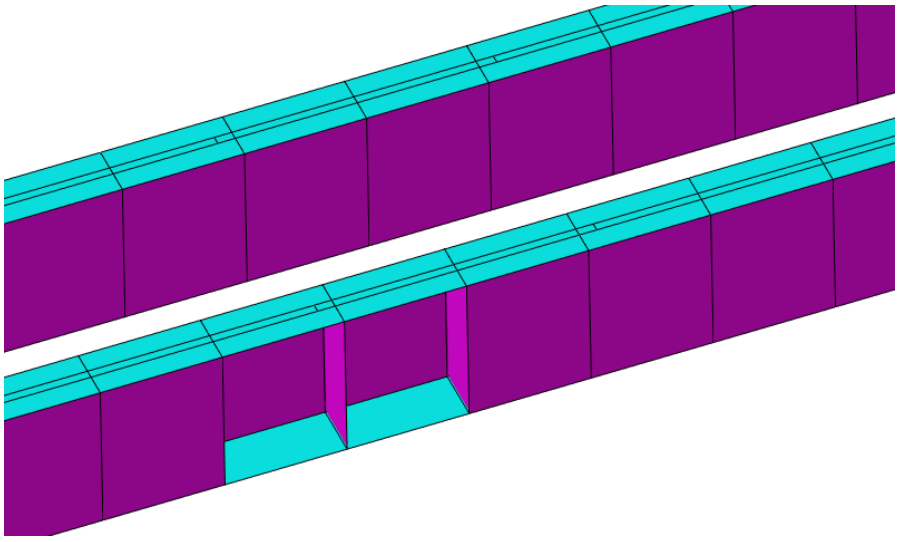

Figure 2. Weld location distribution in bridge frame structure.

3. Numerical methodology and model setup

3.1. Inherent strain method

The inherent strain method is an efficient numerical approach for solving deformation problems in large welded structures. Its core idea is to equate the final effect of the welding process on the structure to an initial strain field, known as the inherent strain field. The welding deformation and residual stress distribution of the structure are then obtained through a single elastic finite element analysis [5]. Unlike the thermal elastoplastic finite element method, which requires tracking the welding thermal-mechanical process step by step, the inherent strain method bypasses the detailed calculation of the intermediate process and directly focuses on the final state after welding [6]. As a result, it greatly reduces computational cost and time, making it particularly suitable for process optimization studies of large and complex welded structures such as bridge cranes. The inherent strain theory holds that the inherent strain ε^* is the sum of the residual components of plastic strain ε_p, thermal strain ε_{th}, transformation strain ε_{tr}, and creep strain ε_c, expressed as [7]:

$$\varepsilon^* = \varepsilon_p + \varepsilon_{th} + \varepsilon_{tr} + \varepsilon_c \tag{1}$$

For large welded structures like crane bridge frames, to determine the transverse and longitudinal inherent strains, the heat input per unit length must first be calculated using welding parameters [8]. The calculation formula is as follows:

$$Q = \frac{\eta UI}{v} \tag{2}$$

where η, U, I, and v are the thermal efficiency, welding voltage, welding current, and welding speed respectively.

Subsequently, the total longitudinal inherent strain Wx and total transverse inherent strain Wy per unit length can be calculated as:

$$W_x = KQ \tag{3}$$

$$W_y = \xi Q \tag{4}$$

where K is the longitudinal inherent strain coefficient, and ξ is the transverse inherent strain coefficient.

According to **Equations (3)** and **(4)**, the longitudinal inherent strain ε_x* and transverse inherent strain ε_y*to be applied are calculated as:

$$\varepsilon_x^* = \frac{W_x}{2ah'} \tag{5}$$

$$\varepsilon_y^* = \frac{W_y}{2ah'} \tag{6}$$

where h' is the plate thickness, and $2a$ is the width of the inherent strain region.

3.2. Heat source calibration

Heat source calibration is performed based on the welding process parameters adopted in the actual production of bridge cranes. The welding method is CO_2 gas shielded arc welding, with an arc voltage of 24 V, welding current of 240 A, welding speed of 5 mm/s, and a thermal efficiency of 0.80. The base material is Q345 steel, which has good weldability and mechanical properties and is commonly used in crane structures. The melting range of Q345 steel is approximately 1400°C to 1500°C. In the temperature field post-processing, areas above 1500°C are uniformly colored to identify the weld pool range.

The calibration object is an 8×10 mm T-joint, using a two-layer two-pass welding process. A double ellipsoid heat source is applied to the finite element model of the T-joint in Sysweld to simulate the temperature field. After calculation, the temperature field distribution of the quasi-steady molten pool is extracted, as shown in **Figure 3(a)**. The shape of the molten pool is observed, and a cross-section perpendicular to the weld direction is taken, as shown in **Figure 3(b)**. The simulation results show that the molten pool is fully penetrated without an obvious lack of fusion. This confirms that the selected double ellipsoid heat source model parameters can accurately reflect the heat input characteristics of the actual welding process. Therefore, the model can be used for subsequent welding sequence simulation of the entire bridge frame.

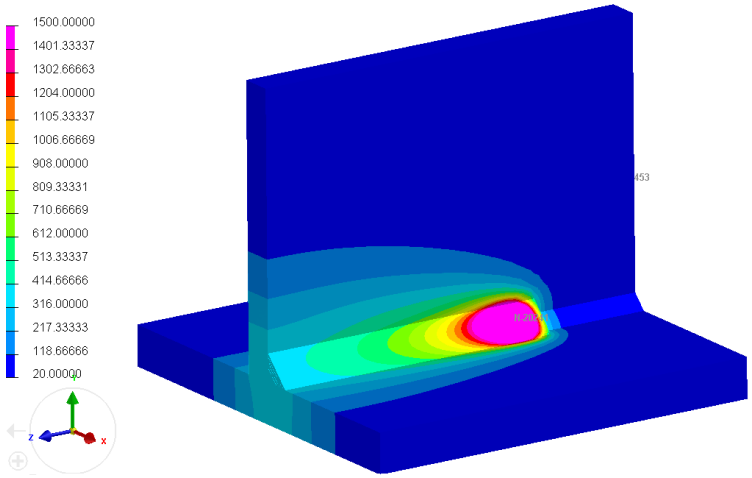

(a) Quasi-steady weld pool shape.

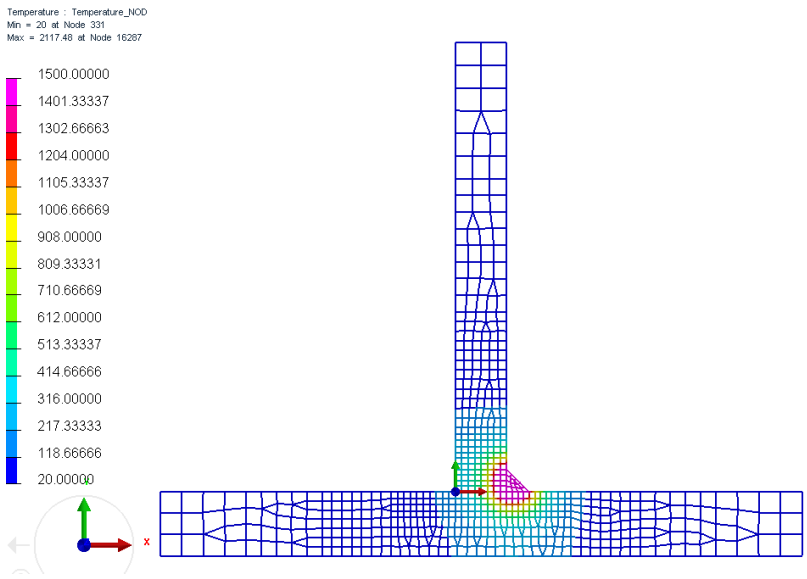

(b) Weld pool cross-section.

Figure 3. Weld pool simulation results.

3.3. Mesh generation of the bridge frame model

First, the mid-surface model of the bridge crane frame structure is established in SolidWorks software. The original model contains many detailed features, such as rounded corners, chamfers, and process bosses, which have negligible influence on welding residual stress analysis and can be omitted. Therefore, these non-critical process features are simplified during modeling, and the mid-surface model suitable for finite element analysis is directly constructed. The model is then imported into Hypermesh for geometry cleanup and meshing, resulting in the finite element model of the bridge frame. After meshing, the total number of elements is 97682, and the number of nodes is 96028. The finite element model is shown in **Figure 4**.

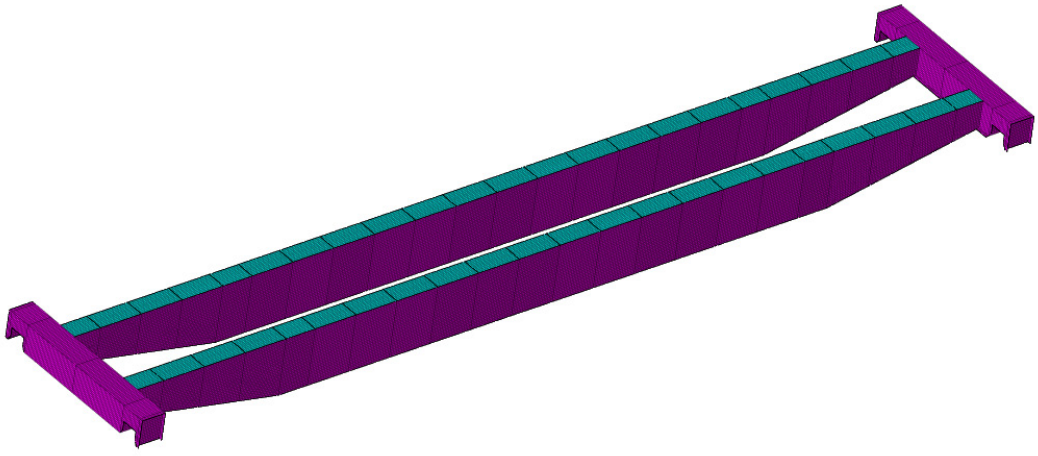

Figure 4. Finite element model of bridge frame structure.

4. Welding sequence simulation schemes and results

4.1. Design of welding sequence schemes

Welding sequence is a key process parameter affecting residual stress and deformation. Different sequences cause differences in the welding process, influence the residual stress of welded joints, and thus change weld quality [9,10]. During welding, the first welds create initial stress and deformation in the structure. This changes the stiffness distribution and constraint state, thereby affecting the stress-strain development of subsequent welds. A reasonable welding sequence can effectively reduce residual stress and deformation. An unreasonable sequence may cause stress and deformation concentration or even increase them. For box-section main beams and end beams, different orders of welding cover plates, stiffener plates, and web plates lead to different results. Based on the geometric characteristics and weld distribution of the bridge crane frame, four different welding sequence schemes are designed. All other process parameters (heat input, clamping conditions, material properties, etc.) remain the same. The four schemes are compared to find the optimal welding sequence.

4.1.1. Scheme 1

First, weld the joints between the top cover plate and the two web plates on one end beam. Then, weld the joints between the top cover plate and stiffener plates on that end beam. Next, process the two main beams in sequence: first weld the joints between the top cover plate and web plates on each main beam, then weld the joints between the top cover plate and stiffener plates. Then, move to the other end beam: first weld the joints between the top cover plate and the two web plates, then weld the joints between the top cover plate and stiffener plates. After that, weld the joints between web plates and stiffener plates on both end beams and main beams. Finally, weld the joints between the bottom cover plate and web plates and stiffener plates on the end beams and main beams.

4.1.2. Scheme 2

First, weld the joints between the top cover plate and web plates on one end beam. Then, weld the joints between the top cover plate and web plates on the two main beams. Next, weld the joints between the top cover plate and web plates on the other end beam. This completes all top cover plate to web plate connections. Then, weld the joints between the top cover plate and stiffener plates on one end beam. Then, weld the joints between the top cover plate and stiffener plates on the two main beams. Finally, weld the joints between the top cover plate and stiffener plates on the other end beam. This completes all top cover plate to stiffener plate connections. Next, weld the joints between web plates and stiffener plates on the end beams and main beams. Finally, weld the joints between the bottom cover plate and web plates and stiffener plates on the end beams and main beams.

4.1.3. Scheme 3

First, complete all welding on one end beam, including the joints between the top cover plate and web plates, between stiffener plates and the top cover plate, web plates, and bottom cover plate, and between the web plates and the bottom cover plate. This end beam becomes a complete box structure. Then, complete all welding on the other end beam, similarly including all joints. Finally, weld the joints between the top cover plate and web plates on the two main beams, then weld the joints between stiffener plates and the top cover plate, web plates, and bottom cover plate, as well as the joints between the web plates and bottom cover plate

on the main beams.

4.1.4. Scheme 4

First, weld the joints between the top cover plate and stiffener plates on one end beam. Then, weld the joints between the top cover plate and the two web plates on that end beam. Next, in sequence, weld the joints between the top cover plate and stiffener plates on each main beam, then weld the joints between the top cover plate and web plates. For the other end beam, again first weld the joints between the top cover plate and stiffener plates, then weld the joints between the top cover plate and web plates. Next, weld the joints between web plates and stiffener plates on the end beams and main beams. Finally, weld the joints between the bottom cover plate and stiffener plates and web plates on the end beams and main beams.

4.2. Simulation results analysis

Simulations are performed in Sysweld according to the four welding sequence schemes. After calculation, residual stress contours, deformation contours, and deformation data in each direction are extracted for systematic comparison. For clarity, the simulation results of Scheme 1 are shown first. The residual stress contour and deformation contour of Scheme 1 are shown in **Figure 5(a)** and **Figure 5(b)**, respectively. From **Figure 5(a)**, the weld and its heat-affected zone are the main areas of residual stress concentration. The maximum residual stress occurs at the weld joint between the top cover plate and stiffener plates on the end beam. From **Figure 5(b)**, the maximum deformation occurs at the junction of the bottom cover plate and web plate of the main beam, located at the middle of the main beam. The maximum total welding deformation is 15.932 mm.

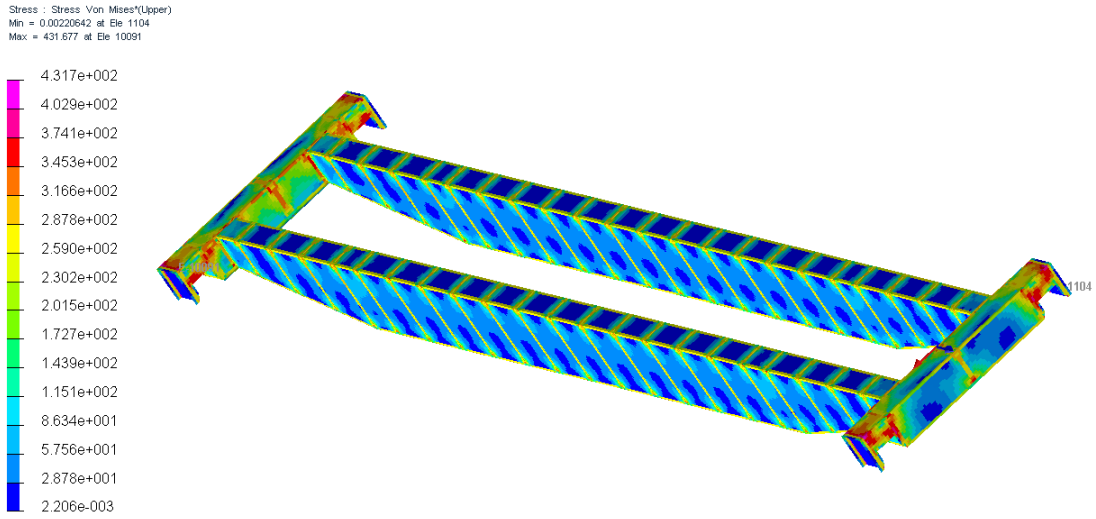

(a) Residual stress contour.

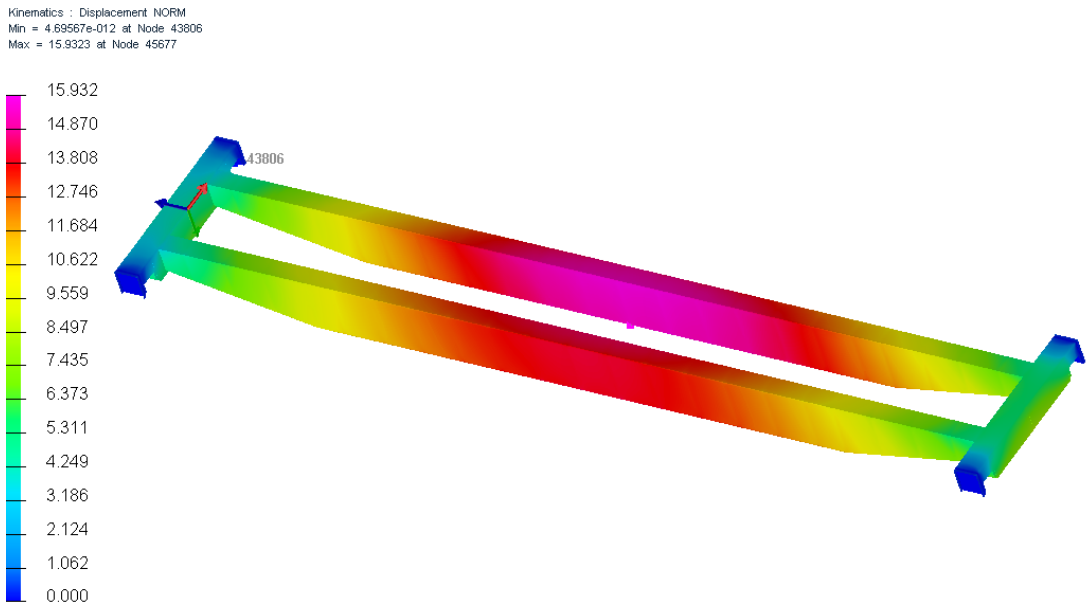

(b) Total residual deformation contour.

Figure 5. Residual stress and deformation contours for Scheme 1.

By observing the simulation result contours of the four schemes, it is found that the distributions of welding residual stress and deformation all show similar patterns. To compare the differences in residual stress and deformation among the four schemes more intuitively, the maximum residual stress data for each scheme are summarized in **Table 1**, and the total residual deformation as well as deformations in the X, Y, and Z directions for each scheme are compiled into a bar chart shown in **Figure 6**.

Table 1. Maximum residual stress for different welding schemes (MPa)

Scheme 1	Scheme 2	Scheme 3	Scheme 4
431.677	432.605	435.235	436.931

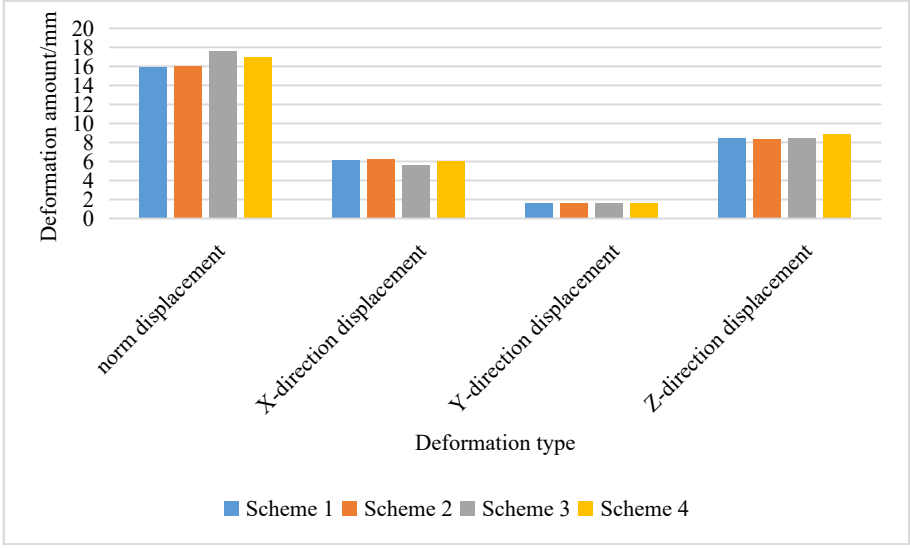

Figure 6. Deformation values for different welding schemes.

Considering both the residual stress and welding deformation simulation results, Scheme 1 has a relatively low peak residual stress among the four schemes. The deformations in the X, Y, and Z directions among the four schemes do not differ significantly, but the total residual deformation of Scheme 1 and Scheme 2 is significantly smaller than that of Scheme 3 and Scheme 4. Since Scheme 1 achieves effective control of both residual stress and deformation, and the welding sequence complies with on-site construction process requirements, Scheme 1 is considered the most reasonable welding sequence among the four schemes.

5. Conclusion

Taking the bridge frame structure of a bridge crane as the research object and based on the inherent strain method, this paper performs numerical simulation analysis of four different welding sequence schemes using the Sysweld welding simulation platform. Through comparative study of residual stress distribution and welding deformation, the following main conclusions are drawn:

(1) The inherent strain method can efficiently complete welding simulation of large and complex bridge frame structures. Under the premise of ensuring accuracy, it greatly improves computational efficiency and is suitable for simulation analysis of crane welded structures;

(2) Heat source calibration is performed on partial T-joints of the bridge frame structure. The final simulation results demonstrate the rationality of the selected heat source model;

(3) Regarding the welding sequence of the structure, welding the longitudinal long welds between webs and cover plates first, followed by the transverse short welds between stiffeners and cover plates, is beneficial for reducing welding residual stress and deformation;

(4) The optimal welding sequence for this bridge crane frame is: first complete the connections between the top plate and webs/stiffeners, then perform the welding between webs and stiffeners, and finally perform the welding between the bottom plate and webs/stiffeners;

Funding

Transportation Science and Technology Plan Project of the Department of Transportation of Liaoning Province (Project No.: 202151)

Disclosure statement

The author declares no conflict of interest.

References

[1] Yuan G, 2023, Failure Modes and Case Analysis of Box Girder of Overhead Crane. Mechanical & Electrical Technology, 2023(1): 98–101.

[2] Yang G, 2023, Research on Welding Residual Stress and Welding Deformation Control Technology of Steel Structures. China Petroleum and Chemical Standard and Quality, 243(12): 156–158.

[3] Wang W, 2010, Optimal Design and Welding Numerical Simulation of Box Girder of Bridge Crane, thesis, Hebei

University of Science and Technology.

[4] Yang Y, Cao X, Li X, et al., 2025, Simulation Study on Effect of Welding Sequence on Welding Deformation. Machinery Manufacturing, 63(7): 79–81,52.

[5] Ren S, Li C, Li L, et al., 2015, Study on Deformation Simulation of Hull Welding based on Inherent Strain Method. Ship Engineering, 37(10): 84–88.

[6] Li Y, Gao F, Jian Z, et al., 2025, Application of Inherent Strain Method in Resistance Spot Welding Deformation Analysis of Large Structures. Welding & Joining, 2025(8): 61–66+83.

[7] Tian L, Liu L, Zhao J, et al., 2025, Numerical Prediction of Welding Deformations in Steel Bridge Deck based on Inherent Strain. Hot Working Technology, 54(23): 132–137+144.

[8] Fan H, Jin C, Li S, et al., 2025, Numerical Simulation of Welding Deformation of Aluminum Alloy Car Body Side Wall based on Inherent Strain Method. Welding Technology, 54(9): 17–21.

[9] Lan L, Shao G, Zhang Y, et al., 2020, Influence of Welding Sequence on Residual Stress and Deformation of T-Joint of Q690 Steel. Journal of Northeastern University (Natural Science), 41(12): 1741–1746.

[20] Liu L, 2023, Influence of Welding Sequence on Residual Stress of Stainless Steel Pipe Welded Joints. Welding Technology, 52(9): 40–43.